ACS SENSORS

pubs.acs.org/acssensors Article

A One-Pot Reverse Transcriptase-Mediated, Pre-amplification-Free CRISPR/Cas12a Assay for Ultrasensitive Nucleic Acid Detection

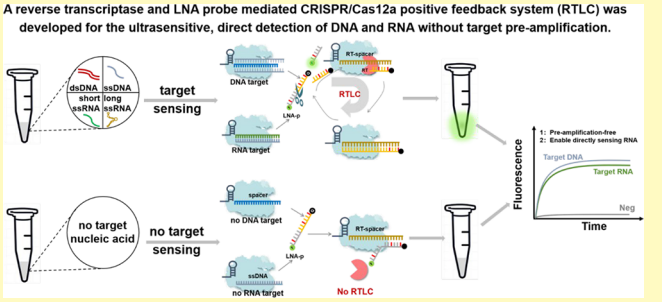
Published as part of ACS Sensors special issue "CRISPR in Sensing".

Ruyi He,[#] Chenchen Zhang,[#] Junqi Zhang, Kaiwen Zhang, Wenhao Yin, Bin Qiao, Luyi Zhang, Shuo Zhang, Jie Qiao,* and Yi Liu*

Cite This: https://doi.org/10.1021/acssensors.6c01202 Read Online

ACCESS | Metrics & More | Article Recommendations | Supporting Information

ABSTRACT: CRISPR/Cas12a holds great promise for biosensing and diagnostics, but conventional methods suffer from low catalytic efficiency, high background, and reliance on pre-amplification. Direct detection of structured RNAs also remains challenging. Herein, we report the development of a reverse transcriptase and LNA probe (LNA-p)-mediated CRISPR/Cas12a positive feedback system (RTLC) for highly efficient, one-pot detection of both DNA and RNA. Without pre-amplification or thermal cycling, the assay achieves a 0.5 aM detection sensitivity within 27 min, exhibits single-base resolution, and allows direct detection of RNAs up to 985 nt in length. Together, RTLC is successfully validated in practical samples by detecting lncRNA HULC and miR-21, offering a robust, versatile tool for high-performance nucleic acid diagnostics.



KEYWORDS: *CRISPR-Cas diagnosis, auto-catalytic, reverse transcriptase, LNA, biomarker detection*

Timely and accurate detection of DNA and RNA is crucial for applications in disease diagnosis, agriculture, food safety, and environmental monitoring.[1,2] However, conventional detection strategies often fail to balance sensitivity, speed, and operational simplicity, severely restricting their application in point-of-care testing. As a revolutionary cutting-edge technology, CRISPR-based diagnostics (CRISPR-Dx) exhibits unparalleled superiority in nucleic acid recognition, positioning it as a powerful candidate for next-generation biosensing tools.[3,4] Despite remarkable progress, the widespread clinical translation of CRISPR-Dx remains hindered by several critical bottlenecks: an ideal detection platform demands not only high sensitivity and specificity, but also facile operation, rapid reaction, and low contamination risk.[5,6]

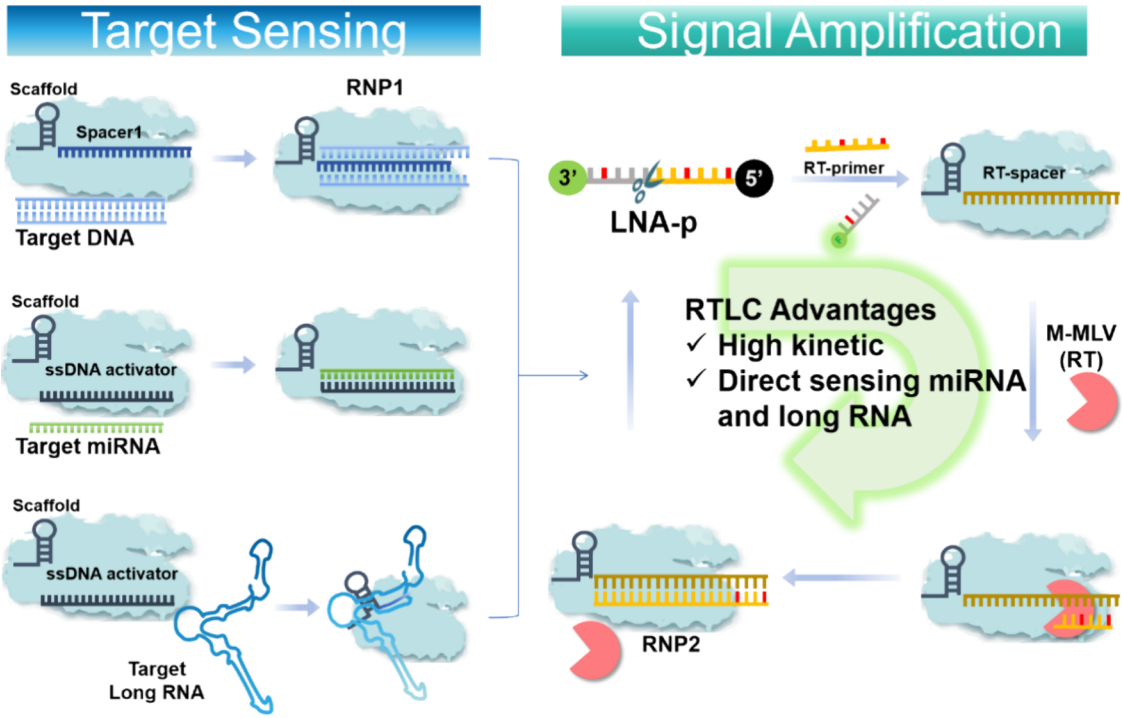
Driven by these practical demands, CRISPR-based detection assays have undergone continuous optimization and upgrading. Early platforms such as SHERLOCK,[7] DETECTR,[8] and HOLMES[9] require two-step reactions, which introduce operational complexity and increase the risk of aerosol contamination. Moreover, Cas12a is often limited to sequence-specific recognition and signal generation only after nucleic acid amplification, thus failing to fully harness its programmable potential. To overcome these drawbacks, diverse strategies have been developed to improve the performance of CRISPR detection systems, including (1) coupling target recognition and Cas12a cleavage with the initiation of isothermal amplification to enable one-pot operation;[10] (2) employing blocker DNA to suppress non-specific *trans*-cleavage and improve detection specificity;[11−13] (3) engineering high-efficiency DNA reporters to enhance Cas12a's *trans*-cleavage activity and sensitivity;[14,15] (4) developing autocatalytic nucleic acid circuits to achieve autonomous signal amplification.[16] Among these, self-catalyzed positive feedback nucleic acid circuits have emerged as a research hotspot owing to their autonomous signal amplification capacity. For instance, the CONAN system[16] and CALSA method[17] have achieved efficient signal amplification via Cas12a-mediated self-catalytic networks, demonstrating promising potential in DNA detection. Nevertheless, these self-catalytic systems are plagued by high background signals stemming from non-specific activation, which is mainly attributed to the nucleic acid "molecular breathing effect", a phenomenon that describes the local, transient, and spontaneous dynamic fluctuation of duplex unwinding and rewinding in double-stranded nucleic acids under physiological conditions.[18,19] However, existing optimization methods involving

Received: March 21, 2026
Revised: August 5, 2026
Accepted: August 6, 2026

Downloaded from pubs.acs.org/ascelj/article-pdf/doi/10.1021/acssensors.6c01202/6604899/se-2026-01202n.pdf by XIAMEN UNIV user on 23 August 2026

ACS Publications © XXXX American Chemical Society

Scheme 1. Schematic Illustration of the Direct Detection of DNA, miRNA, and Long RNA Using the RTLC Reaction System[a]



[a]LNA-P: LNA-modified probes, RT: reverse transcriptase, RNP: Cas12a ribonucleoprotein complex.

chemical modifications and specialized treatments inevitably increase system complexity and decelerate reaction kinetics.[20]

Beyond the above limitations, direct RNA detection—particularly for long RNA molecules with intricate secondary structures—remains a formidable challenge, rooted in Cas12a's intrinsic DNA-preferred recognition property. Although Cas13a enables direct RNA targeting, its clinical application is constrained by poor tolerance to RNA length, severe interference from secondary structures, and unstable RNA reporters.[21−23] To address this dilemma, researchers have developed a "split activation" strategy to engineer the Cas12a system for direct RNA detection,[24−26] For example, our group previously constructed a functionally active split crRNA comprising a 5′scaffold and a 3′spacer, establishing the SCas12a method for direct RNA recognition; target RNA acts as a functional spacer to hybridize with the scaffold and trigger Cas12a-mediated signal amplification.[24,25] Similarly, the SAHARA technology employs a proximal/distal split nucleic acid architecture to activate Cas12a *trans*-cleavage, realizing picomolar-level RNA detection.[26] Recently, a proximity-assembly and activation (PAA) strategy[27] and a biosensor based on dynamic reassembly of crRNA scaffold[28] have been developed to further optimize the split crRNA–based CRISPR/Cas12a diagnostic system, achieving highly sensitive detection of miRNAs and small molecules. Meanwhile, deep learning has advanced rapidly in biosensing data analysis, serving as a powerful tool for extracting weak, high-dimensional features from complex signals[29,30] and showing great potential in boosting the performance of CRISPR-based diagnostic systems.[31] Nevertheless, these methods still face challenges in detecting RNAs at extremely low concentrations or long RNA molecules with complex secondary structures.

In this study, by leveraging the modular design of split-crRNA, we developed a reverse transcriptase and LNA probe-mediated CRISPR/Cas12a positive feedback system, termed RTLC (Scheme 1). This system enables continuous generation of activated Cas12a ribonucleoprotein complexes (RNPs) in a one-pot reaction, allowing for highly sensitive and specific detection of diverse nucleic acids. The initial target serves as a direct trigger for the first-round activation of Cas12a. Upon target recognition, Cas12a is activated and *trans*-cleaves the LNA probe, releasing its 3′ end to serve as a reverse transcription (RT) primer. Reverse transcriptase extends this primer using the spacer RNA as a template, producing DNA-RNA hybrid duplexes that activate the Cas12a-scaffold complex. This triggers further cleavage of the LNA probe, initiating a positive feedback loop. Throughout the entire reaction, no fully complementary double-stranded nucleic acid structures exist in the system. This design fundamentally eliminates the local transient unwinding-rewinding fluctuation known as molecular breathing. We initially evaluated widely used *As*Cas12a and *Lb*Cas12a for RTLC implementation, but observed elevated background activity. Upon switching to the *Ct*Cas12a, which is derived from the thermophilic bacterium *Clostridium thermobutyricum*,[32] we found significantly lower background and a higher signal-to-noise ratio, leading to its exclusive adoption in all subsequent experiments.

With this optimized system, RTLC enables direct detection of various nucleic acids, including dsDNA, ssDNA, miRNA, and long RNA, by only providing the complementary nucleic acid activator. The highly efficient self-catalytic system allows for detection at concentrations as low as 0.5 aM within 27 min, representing a 10^6-fold improvement over conventional Cas12a systems.[33] We further validated the practical application

https://doi.org/10.1021/acssensors.6c01202
ACS Sens. XXXX, XXX, XXX−XXX

Downloaded from pubs.acs.org/ascelj/article-pdf/doi/10.1021/acssensors.6c01202/6604899/se-2026-01202n.pdf by XIAMEN UNIV user on 23 August 2026

potential of RTLC by successfully detecting long non-coding RNA HULC in liver cancer cells (HepG2) and miR-21 in colorectal cancer patient samples. Collectively, the RTLC system features user-friendliness and sequence programmability, while addressing the longstanding challenges in detecting RNAs with complex secondary structures and highlighting the application value of novel Cas12a variants. As such, it represents a highly efficient and promising tool for high-sensitivity, high-specificity nucleic acid diagnostics.

■ RESULTS AND DISCUSSION

Design and Construction of the RTLC System

Current Cas12a-based positive-feedback circuits suffer several prominent limitations: complicated molecular construction, unsatisfactory performance in direct RNA detection, and low sensitivity for long RNA with complex higher-order structures.[16,17,20] To tackle these bottlenecks, we constructed a CRISPR/Cas12a positive-feedback system (RTLC) integrated with reverse transcriptase and locked nucleic acid (LNA) probes. This one-pot assay is pre-amplification-free, which refers to no independent external target amplification (PCR, LAMP, etc.) before CRISPR reaction and enables ultrasensitive detection of various nucleic acid targets. Signal amplification in the RTLC reaction primarily arises from the LNA-modified probes, reverse transcriptase activity, and the Cas12a-mediated positive feedback loop. The system is designed to avoid non-specific activation caused by nucleic acid conformational changes, a major flaw in previously reported self-catalytic circuits.[17,20,34]

We firstly evaluated the efficiency of primers of varying lengths in initiating reverse transcription (Figure 1A, Table S2). A 6-nucleotide primer effectively triggers the reaction (Figure S1), generating a sufficient amount of DNA-RNA hybrid duplex. This product directly activates Cas12a-Scaffold, whereas longer primers do not significantly enhance activity (Figure 1B). Therefore, we selected the 6-nt primer for use in RTLC. To assess system compatibility, we tested the integration of the reverse transcription and Cas12a reaction systems using rCutSmart buffer, RT buffer, and a 1:1 mixture of both (Figure S2), with full-length ssDNA activator as the positive control. The results show that rCutSmart alone supports reaction kinetics and fluorescence output comparable to the positive control, demonstrating that Cas12a detection and reverse transcription can proceed simultaneously in a single reaction tube.

According to the previous study,[17] when the 5′-terminal positions 1, 4, and 10 of the 11-nt single-stranded DNA probe are modified with LNA, the trans-cleavage sites of Cas12a are precisely restricted between the 6th and 5th nucleotides. To ensure precise generation of the 6-nt RT primer via Cas12a collateral cleavage, we adopted the design described above (Table S3). The 11-nt ssDNA probe was labeled with 5′-BHQ1 and 3′-FAM, and LNA modifications were introduced at the three specific positions (Figure 1C). This design restricts Cas12a's *trans*-nuclease cleavage to a defined site, producing two fixed fragments: a 5-nt fragment (5′-TTAAC-3′-FAM) and a 6-nt fragment (BHQ1-5′-GAACGC-3′), the latter of which acts as the RT primer to initiate the positive feedback loop. High-resolution PAGE analysis confirmed that cleavage of the LNA-modified probe by different nucleic acid targets (ssDNA, dsRNA, RNA) or different Cas12a orthologs (*As*Cas12a, *Lb*Cas12a, *Ct*Cas12a) produced the same defined ssDNA products (Figures 1D and S3). Previous studies have shown that replacing DNA primers with LNA-enhanced primers can significantly enhance the binding stability with the target RNA. More

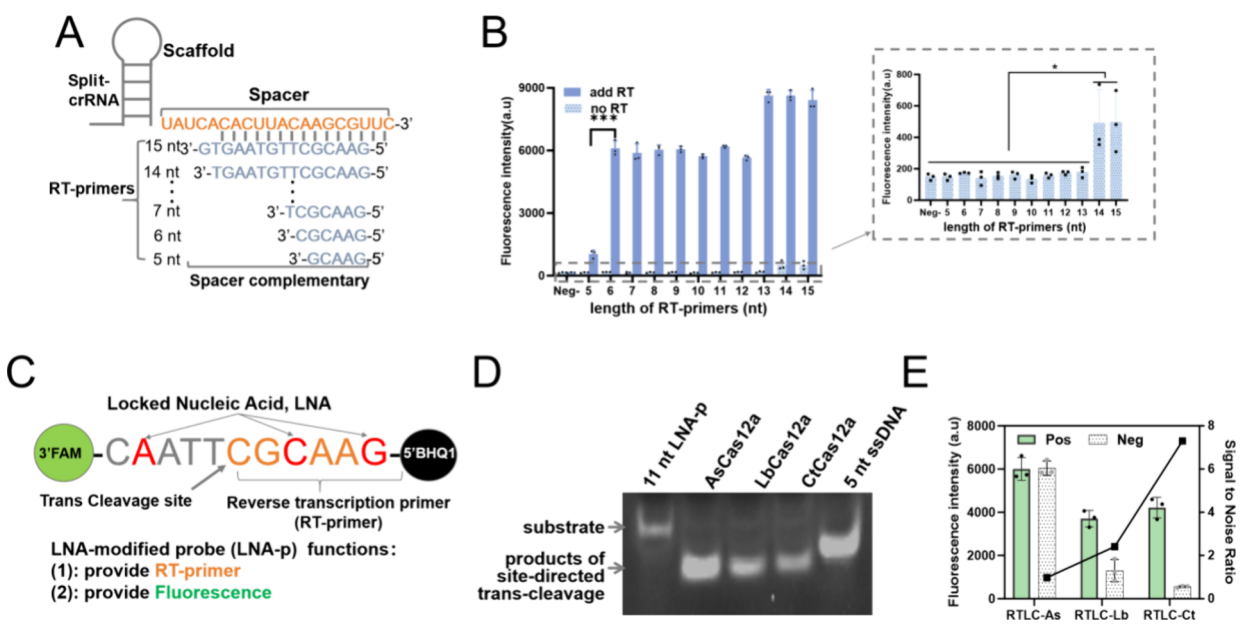


Figure 1. Selection of reverse transcription primer and LNA-modified probe. (A) Schematic design of primers used for reverse transcription, ranging in length from 5 to 15 nucleotides. (B) Fluorescence signals generated by reverse transcription using primers of varying lengths. $n = 3$ independent experiments. ***$P < 0.001$, ****$P < 0.0001$, based on two-tailed *t*-tests. (C) Design of the LNA-modified probe. (D) High-resolution PAGE analysis (without staining) of trans-cleavage products generated by three Cas12a orthologs on the LNA-modified probe. (E) Detection results for AsCas12a, LbCas12a, and *Ct*Cas12a used in the RTLC method. "Pos" and "Neg" stand for positive and negative, respectively. Data are presented as mean ± SD ($n = 3$).

Downloaded from pubs.acs.org/ascelj/article-pdf/doi/10.1021/acssensors.6c01202/6604899/se-2026-01202n.pdf by XIAMEN UNIV user on 23 August 2026

https://doi.org/10.1021/acssensors.6c01202
ACS Sens. XXXX, XXX, XXX−XXX

importantly, this modification can be efficiently recognized and extended by reverse transcriptases (including M-MLV-derived enzymes), especially when dealing with highly structured or ultra-short sequences.[35,36] These findings validate the LNA-modified probe as a reliable "switch" element for the RTLC circuit. Notably, the LNA-mediated precise probe cleavage, combined with the intrinsic sequence specificity requirement of reverse transcriptase for primer recognition, effectively circumvents the core flaw of previously reported self-catalytic Cas12a systems: single-stranded activators containing pendant structures can activate Cas12a's trans-cleavage activity to varying degrees.[34,37] Such as, in the CALSA assay,[17] conformational fluctuations of H0 molecules during the process of reaching dynamic equilibrium may promote the formation of unintended pendant activators through interaction with LNA-ss4, thereby inadvertently triggering the cascade reaction.

We further compared the fluorescence signals and signal-to-noise ratio (SNR), the ratio of the fluorescence signals at the positive and negative endpoints, of three widely used Cas12a orthologs (*As*Cas12a, *Lb*Cas12a, *Ct*Cas12a) in the RTLC system. *As*Cas12a failed to distinguish between positive and negative samples, with negligible signal discrimination (Figures 1E and S4A,D,E). *Lb*Cas12a enabled clear target detection but exhibited a high baseline background and a low SNR (Figures 1E and S4B,D,E). In contrast, *Ct*Cas12a exhibited excellent target discrimination and a markedly improved SNR (Figures 1E and S4C–E). This finding is consistent with previous reports of non-specific collateral activity in wild-type *As*Cas12a and *Lb*Cas12a, and despite the widespread use of *Lb*Cas12a in one-tube detection assays,[16,17,20,38,39] our data demonstrate that *Ct*Cas12a is uniquely suited for the RTLC system due to its low background and high activation specificity. Furthermore, TBE-PAGE analysis with FAM-labeled LNA probes validated the successful formation of RNA-DNA hybrids in the RTLC system (Figure S5).

To validate the signal amplification advantage of RTLC, we compared the performance of the LNA probe-driven RTLC assay, a DNA probe (unmodified) control RTLC assay, and the conventional single Cas12a reaction (SCas12a) (Figure 2A). At high ssDNA target concentrations (10 nM), all three systems generated strong fluorescence signals. However, at low target concentrations (10 pM), only the LNA-p-driven RTLC assay produced robust, detectable signals (Figure 2B–G). The unmodified DNA probe displayed low binding stability and non-specific random cleavage (Figure S6), which decreased the yield of functional 6-nt RT primer and impaired subsequent extension, thus breaking the positive feedback loop. This performance trend was consistent cross dsDNA and RNA target detection (Figure S7), confirming that the LNA-modified probe is critical for the high sensitivity and autocatalytic efficiency of the RTLC system.

Optimization of Reaction Conditions for the RTLC Assay

To maximize the reaction speed, fluorescence intensity, and SNR of the RTLC assay, we systematically optimized key reaction parameters, including the molar ratio and concentration of Cas12a and crRNA scaffold, RT concentration, dNTP concentration, L-proline (L-pro) concentration, and supplementary Mg^{2+} concentration. All optimizations were performed using ssDNA as the positive control and nuclease-free water as the negative control, with fluorescence signals measured at the 15-min time point to improve the performance (Figure 3).

Using a fixed scaffold concentration of 1 μM, we first titrated the Cas12a: Scaffold molar ratio, finding that a 2:1 ratio yielded the highest SNR (Figure 3A). We then optimized the absolute concentrations at this fixed ratio, selecting 2 μM Cas12a and 1 μM scaffold for subsequent experiments (Figures 3B and S8). For the RT reaction, 0.2 U/μL of M-MLV reverse transcriptase and 25 μM dNTPs achieved the optimal balance of SNR and reagent cost (Figure 3C,D). Meanwhile, we found that supplementation with 100 mM L-pro and 20 mM additional Mg^{2+} further enhanced the signal amplification efficiency and specificity of the RTLC system (Figure 3E,F). It has been well documented that L-pro boosts the cleavage activity and reaction stability of Cas12a by stabilizing its protein conformation,[40] while Mg^{2+}, as an essential cofactor for Cas12a nuclease activity, significantly promotes its *cis*-and *trans*-cleavage by stabilizing the R-loop complex conformation.[41] These optimized conditions were used for all subsequent experiments. In summary, the key optimized reaction parameters were as follows: the Cas12a: scaffold molar ratio was set to 2:1, with absolute concentrations of 2 μM Cas12a and 1 μM scaffold; the reverse transcription system used 0.2 U/μL M-MLV reverse transcriptase and 25 μM dNTPs; and the reaction was supplemented with 100 mM L-proline and an additional 20 mM Mg^{2+}. These optimized conditions were utilized for all subsequent experiments.

High-Sensitivity and Versatility of the RTLC Assay for Nucleic Acid Detection

We further applied the optimized RTLC assay to detect diverse nucleic acid targets, including ssDNA, dsDNA, and miRNA. Target-specific RNP1 workflows were designed as illustrated in Figure 4A–C. Notably, the RNP2 complex remained unaltered, and only the spacer sequence within RNA1 or the ssDNA activator was adjusted to match the corresponding target. As shown in Figure 4D–F, Fluorescence signals across the target concentration range of 0.5 aM to 10 pM were higher than the negative control ($P < 0.05$). In our study, the limit of detection (LOD) was determined based on a 3σ criterion: threshold = $\text{Mean}_{NTC} + 3\text{SD}_{NTC}$ with a corresponding SNR threshold. To statistically verify whether the observed signals were genuine target-specific cleavages rather than random background fluctuations, we performed 12 independent replicates for both the 0.5 aM ssDNA target and the negative controls (NTC) to ensure statistical power for low-abundance detection. At 27 min, the 0.5 aM group achieved a 100% detection rate with an average SNR of 2.31, which is well above the calculated SNR threshold of 1.68 (Figure S9, Table S1).

Furthermore, analysis of SNR across the entire concentration range at 15, 30, and 50 min (Figure S10) consistently met these criteria. The assay maintained sustained amplification with low background over 50 min (Figure 4G–I). For miRNA targets, a slight lag (~20 min) was observed before signal accumulation, consistent with their structural characteristics. These results demonstrate that the RTLC assay offers high versatility and ultra-high sensitivity, enabling reliable detection of diverse nucleic acids down to 0.5 aM.

Specificity of the RTLC Assay for miRNA Detection

Given that *Ct*Cas12a is an atypical Cas12a ortholog, we initially assessed its tolerance to single-base mutations in miRNA targets via a split crRNA strategy. As illustrated in Figure 5A,B, *Ct*Cas12a displayed high discrimination capacity

Downloaded from pubs.acs.org/ascelj/article-pdf/doi/10.1021/acssensors.6c01202/6604899/se-2026-01202n.pdf by XIAMEN UNIV user on 23 August 2026

https://doi.org/10.1021/acssensors.6c01202
ACS Sens. XXXX, XXX, XXX–XXX

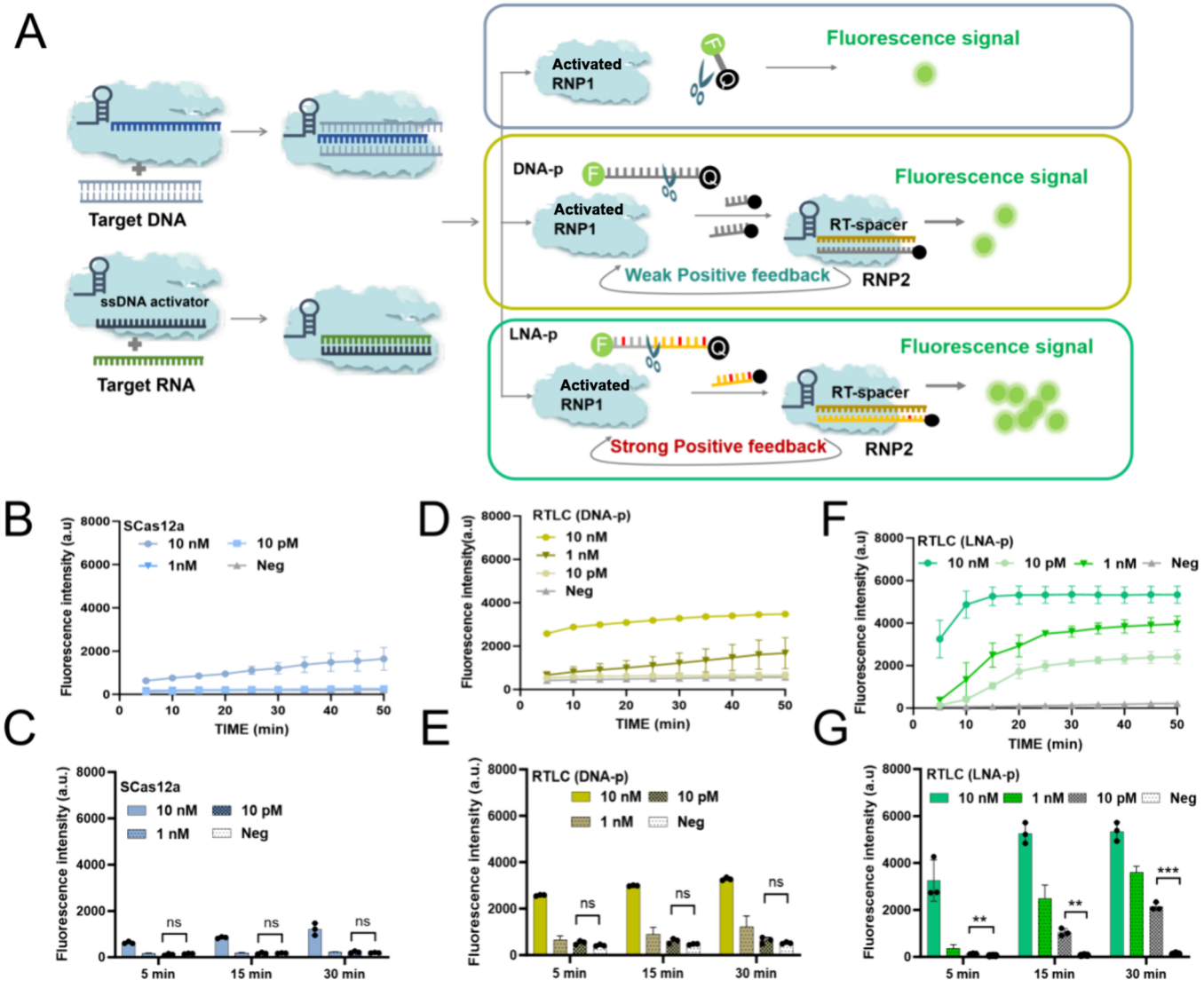


Figure 2. Comparison between the single Cas12a and RTLC reactions mediated by probes with or without LNA modification. (A) Schematic illustration of conventional Cas12a reaction, and RTLC using DNA-p or LNA-p. Real-time fluorescence kinetic curve of the conventional Cas12a reaction (B), RTLC using DNA-p (D), and RTLC using LNA-p (F) for detecting 10 nM, 1 nM, and 10 pM ssDNA targets. End-point fluorescence values from the conventional Cas12a reaction (C) RTLC using DNA-p (E) and RTLC using LNA-p (G) for detecting 10 nM, 1 nM, and 10 pM ssDNA targets. Data are presented as mean ± SD ($n = 3$). Statistical significance is indicated as follows: $^{*}P < 0.05$, $^{**}P < 0.01$, $^{***}P < 0.001$, $^{****}P < 0.0001$, based on two-tailed *t*-tests.

for single-point mutations at most nucleotide positions of the target miRNA, with prominent recognition efficiency for mutations at positions 1, 2, 5, 10, 15–17, and 19–21. To further verify the ability of RTLC for low-abundance miRNA mutation detection, we prepared mixed samples containing M15 (Figure 5C) and M19 (Figure 5D) mutants at frequencies of 1, 0.1, 0.01, and 0% against a wild-type miR-21 background, respectively. The corresponding results confirmed that the RTLC assay can effectively discriminate mutant miRNAs with an abundance as low as 0.01%, underscoring its promising application potential in RNA mutation analysis.

Detection of Long RNA Using the RTLC Assay

Direct detection of long RNA molecules remains a major challenge for Cas12a-based assays.[21,24–26] Whiting and Champoux[42] had confirmed that Moloney murine leukemia virus (MLV) reverse transcriptase possesses strand displacement activity. When dealing with complex templates such as RNAs containing secondary structures, they can still maintain stable synthetic activity. On the other hand, Several commercially available reverse transcriptases have shown significant improvements in stability, synthesis rate, and adaptability to complex RNA templates, and have been widely used in various research studies, such as BeyoRT II M-MLV reverse transcriptase (RNase H-) (D7160S) in this study.

We therefore evaluated the performance of the RTLC assay for detecting long RNA fragments of varying lengths (Table S4 and Figure S11): an 86 nt HCV RNA fragment (Figure S12), a 100 nt lncRNA HULC fragment (Figure 6), a 150 nt P53 RNA fragment (Figure S13), and a 985 nt SARS-CoV-2 RNA fragment (Figure S14). The range (86–985 nt) covers the lengths of many pathogen-derived RNAs, mRNAs,

https://doi.org/10.1021/acssensors.6c01202
ACS Sens. XXXX, XXX, XXX–XXX

Downloaded from pubs.acs.org/ascelf/article-pdf/doi/10.1021/acssensors.6c01202/6604899/se-2026-01202n.pdf by XIAMEN UNIV user on 23 August 2026

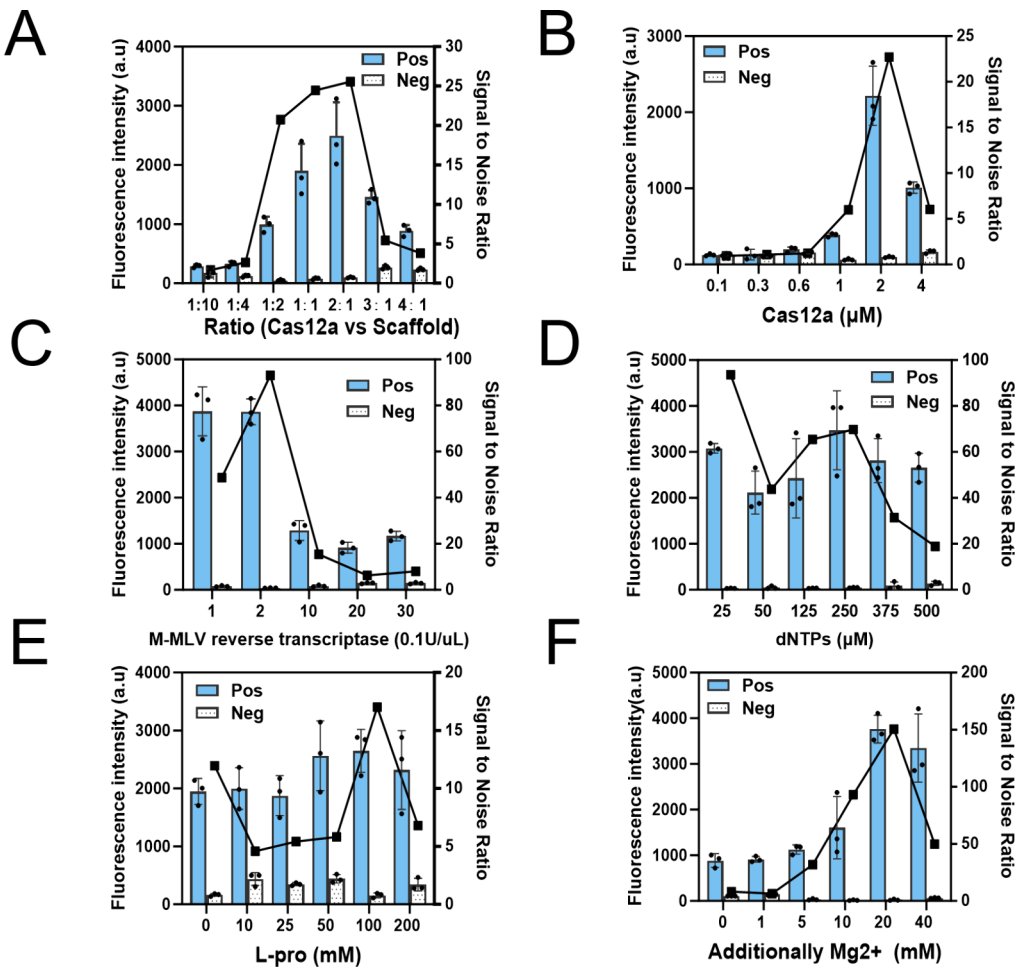


Figure 3. Optimization of RTLC reactions. (A) Titration of the Cas12a: Scaffold ratio at a fixed scaffold concentration of 1 μM. (B) Titration of Cas12a concentration at a fixed Cas12a: Scaffold ratio of 2:1. (C) Titration of M-MLV reverse transcriptase concentration at a fixed Cas12a:Scaffold ratio of 2 μM:1 μM. (D) Titration of dNTP concentration at a fixed Cas12a:Scaffold ratio of 2 μM:1 μM and M-MLV reverse transcriptase concentration of 0.2 U/uL. (E) Titration of L-pro concentration under fixed conditions: Cas12a:Scaffold (2 μM:1 μM), M-MLV reverse transcriptase (0.2 U/uL), and dNTPs (25 μM). (F) Titration of additional Mg^{2+} concentration."Pos" and "Neg" stand for positive and negative, respectively. Data are presented as mean ± SD ($n = 3$).

and long non-coding RNAs. For each target, we designed ssDNA activators targeting three randomly selected binding sites.While the RTLC system successfully detected all tested sites—even within regions predicted to form stable secondary structures (Figures 6A–C and S12–S14)—we observed variable signal intensities across different sites, which we attribute to differences in local RNA secondary structure that affect activator hybridization efficiency. Notably, this site-to-site variability has minimal impact on qualitative detection but may introduce deviations in absolute quantification. For optimal performance, we recommend selecting binding sites with predicted single-stranded regions via bioinformatic tools, followed by small-scale experimental validation to identify the site with the highest signal-to-noise ratio (SNR). Subsequently, we selected the ssDNA activator yielding the highest SNR to evaluate the sensitivity of RTLC for long RNA detection and found that it can detect targets at concentrations as low as 0.5 aM within 15–60 min (Figures 6D–F and S15). Based on this results, we hypothesize that this RT promotes efficient hybridization of the ssDNA activator to stem-loop regions of the target RNA, forming DNA-RNA heteroduplexes that recruit the Cas12a-scaffold complex and trigger trans-cleavage. Our results demonstrate the versatility of the RTLC system for detecting diverse RNA targets of biological and clinical relevance.

Application of the RTLC Assay in Practical Scenarios

The practical workflow of the RTLC assay is depicted in Figure 7A. In drug development, long non-coding RNAs (lncRNAs) specifically overexpressed in tumor cell lines serve as promising therapeutic targets.[43] Accurate quantification of their expression dynamics enables validation of drug regulatory effects, accelerates related research and development processes, and facilitates the discovery of lncRNA-targeted antitumor therapies. Among these lncRNAs, lncRNA HULC is highly overexpressed in hepatocellular carcinoma (HCC) and closely linked to tumor drug resistance.[44,45] Accordingly, we extracted total RNA from cultured HepG2 and HEK293T cells and employed the RTLC assay to detect HULC expression levels. Receiver operating characteristic (ROC) curve analysis was performed using 27 positive and 27 negative samples, establishing an SNR threshold of 1.676 (Figure 7B,C). This optimal threshold endowed the assay with 100% sensitivity and 100% specificity.

Downloaded from pubs.acs.org/ascelj/article-pdf/doi/10.1021/acssensors.6c01202/6604899/se-2026-01202n.pdf by XIAMEN UNIV user on 23 August 2026

https://doi.org/10.1021/acssensors.6c01202
ACS Sens. XXXX, XXX, XXX–XXX

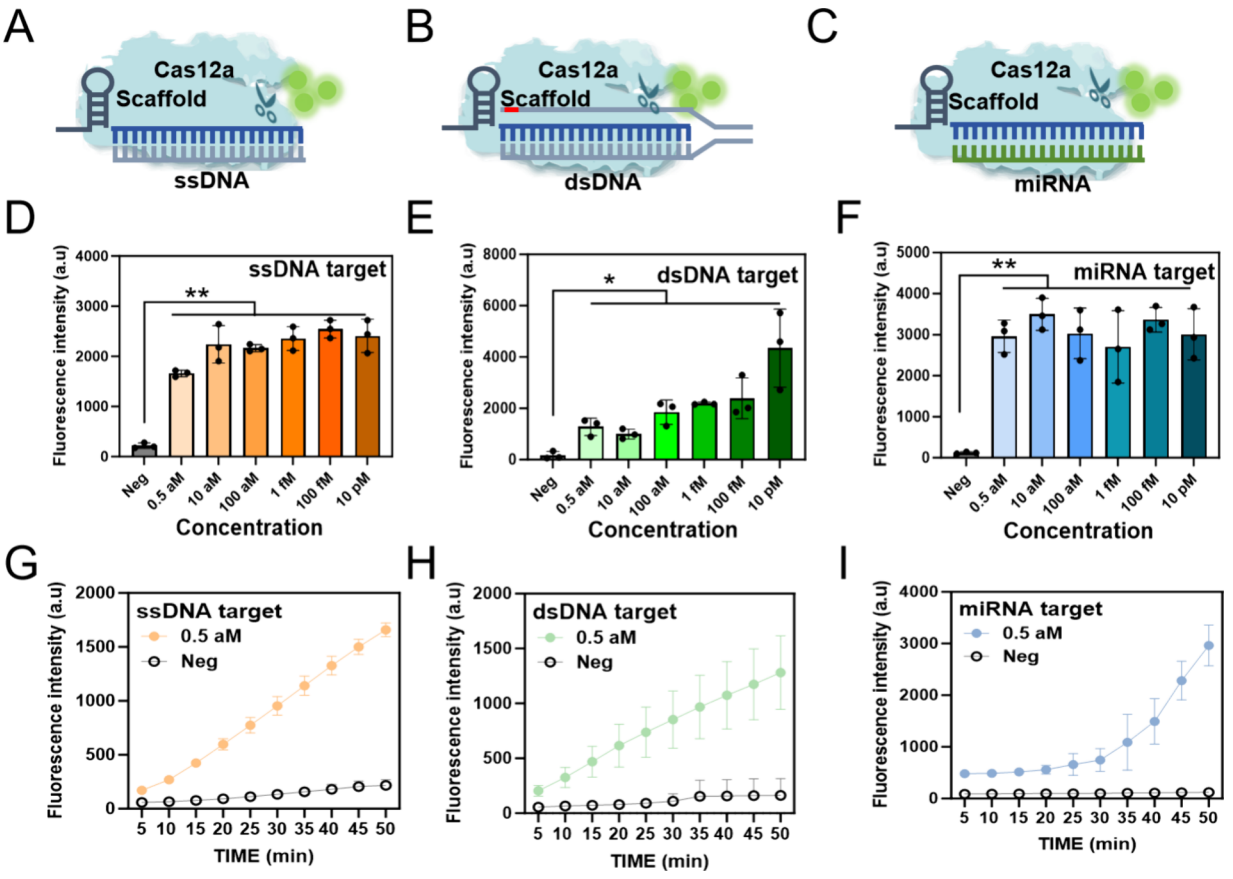


Figure 4. Sensitivity evaluation of RTLC for detecting different types of nucleic acid targets. (A–C) Schematic illustrations of Cas12a recognition of various nucleic acid targets: (A) ssDNA, (B) dsDNA, and (C) miRNA. (D–F) Fluorescence intensity for each target type detected over 50 min across a concentration range: (D) ssDNA, (E) dsDNA, and (F) miRNA. (G–I) Real-time fluorescence kinetic curve 0.5 aM target: (G) ssDNA, (H) dsDNA, and (I) miRNA. "Neg" stands for negative. Data are presented as mean ± SD ($n = 3$). Statistical significance is indicated as follows: $^{**}P < 0.01$, based on two-tailed t-tests.

For clinical diagnosis, miR21 is one of the earliest identified microRNAs with aberrantly high expression in various solid tumors.[46] We collected peripheral blood samples from 12 colon cancer patients and 8 healthy volunteers, extracted miRNAs from equal volumes of plasma via a standard protocol according to miRcute miRNA Isolation Kit (TIANGEN; DP503), and quantified miR-21 levels using the RTLC assay. The results demonstrated that miR21 was significantly overexpressed in the peripheral blood of colon cancer patients compared with the healthy group (Figure 7D,E), which validated the clinical applicability of the established assay.

■ CONCLUSIONS

In summary, we developed a novel positive-feedback nucleic acid detection system termed RTLC, which integrates Cas12a, split crRNA, reverse transcriptase, and LNA-modified probes in a one-pot format without pre-amplification. Compared with existing methods, RTLC exhibits three prominent merits (Table S5): first, it delivers 0.5 aM sensitivity within 27 min without nucleic acid pre-amplification, and enables detection of 0.01% low-abundance mutations, greatly improving detection efficiency and convenience; second, it features broad applicability for diverse nucleic acid targets, including ssDNA, dsDNA, miRNA and long-chain RNA; third, its simple activator design avoids interference from molecular breathing effects, guaranteeing robust system stability. Furthermore, RTLC has demonstrated rapid and reliable detection of lncRNA HULC and miR-21 in real biological samples. Notably, RNA pre-extraction is still required for serum sample detection. Future efforts will focus on integrating this autocatalytic system with simplified sample preparation strategies that eliminate the need for conventional nucleic acid extraction and purification. In addition, the positive-feedback loop continuously generates DNA-RNA hybrid amplicons that sustain persistent Cas12a activation, which introduces potential laboratory carryover contamination risks analogous to PCR. This risk mignt be mitigated via potential strategies such as UDG digestion and physically separated experimental zones. In summary, RTLC surmounts the drawbacks of traditional pre-amplification strategies, offering a sensitive and specific platform for clinical point-of-care diagnostics, underscoring its strong potential for clinical applications.

■ ASSOCIATED CONTENT

Supporting Information

The Supporting Information is available free of charge at https://pubs.acs.org/doi/10.1021/acssensors.6c01202.

Downloaded from pubs.acs.org/ascefj/article-pdf/doi/10.1021/acssensors.6c01202/6604899/se-2026-01202n.pdf by XIAMEN UNIV user on 23 August 2026

https://doi.org/10.1021/acssensors.6c01202
ACS Sens. XXXX, XXX, XXX–XXX

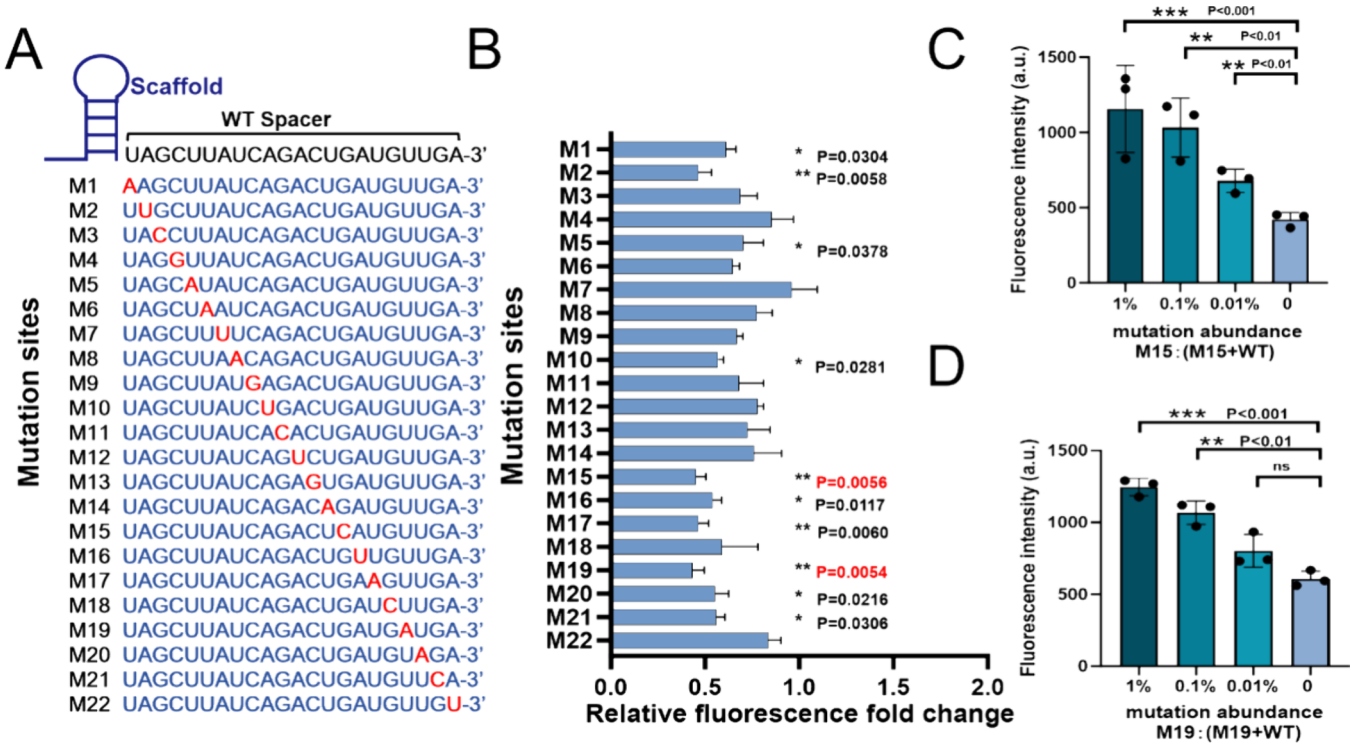


Figure 5. Specificity of the RTLC assay for miRNA detection. (A) Spacers were designed with point mutations introduced across the pairing region of the miR21 target. (B) Fluorescence fold changes from *Ct*Cas12a *trans*-cleavage activity. All fluorescence values were normalized to those obtained from the wild-type (WT) miR-21 target. Fluorescence signals of RTLC detection for simulated miRNA samples with the mutant at position 15 (C) or 19 (D) in a background of wild-type miRNA. Data are presented as mean ± SD ($n = 3$). Statistical significance is indicated as follows: ns, not significant, $^{**}P < 0.01$,$^{***}P < 0.001$, based on two-tailed *t*-tests.

Ethical statement; materials; recombinant Cas12a orthologs protein expression and purification; gel electrophoresis; single Cas12a assay; application of the RTLC fluorescence assay for DNA and RNA detection; cell culture and lncRNA HULC detection; miRNA detection of human plasma samples; supplementary figures (Figures S1–S15); supplementary tables (Tables S1–S5); and SI references (DOCX)

■ AUTHOR INFORMATION

Corresponding Authors

Jie Qiao – *School of Life Science and Technology, Wuhan Polytechnic University, Wuhan, Hubei 430023, China;* Email: jieqiao@whpu.edu.cn

Yi Liu – *State Key Laboratory of Biocatalysis and Enzyme Engineering, School of Life Sciences, Hubei University, Wuhan, Hubei 430042, China; BravoVax Co., Ltd., Wuhan, Hubei 430075, China;* orcid.org/0000-0002-2148-3596; Email: yiliu0825@hubu.edu.cn

Authors

Ruyi He – *School of Life Science and Technology, Wuhan Polytechnic University, Wuhan, Hubei 430023, China*

Chenchen Zhang – *School of Life Science and Technology, Wuhan Polytechnic University, Wuhan, Hubei 430023, China*

Junqi Zhang – *State Key Laboratory of Biocatalysis and Enzyme Engineering, School of Life Sciences, Hubei University, Wuhan, Hubei 430042, China*

Kaiwen Zhang – *School of Life Science and Technology, Wuhan Polytechnic University, Wuhan, Hubei 430023, China*

Wenhao Yin – *State Key Laboratory of Biocatalysis and Enzyme Engineering, School of Life Sciences, Hubei University, Wuhan, Hubei 430042, China*

Bin Qiao – *Department of Oral and Maxillofacial Surgery, The First Affiliated Hospital of Zhengzhou University, Zhengzhou University, Zhengzhou 450001, China*

Luyi Zhang – *School of Life Science and Technology, Wuhan Polytechnic University, Wuhan, Hubei 430023, China*

Shuo Zhang – *School of Life Science and Technology, Wuhan Polytechnic University, Wuhan, Hubei 430023, China*

Complete contact information is available at: https://pubs.acs.org/doi/10.1021/acssensors.6c01202

Author Contributions

#R.H. and C.Z. contributed equally to this work. J.Q., R.H., and Y.L. designed research; R.H., C.Z., J.Z., L.Z., S.Z., and K.Z. performed research; W.Y. and B.Q. collected the patient samples; R.H., C.Z., and Y.L. analyzed data; R.H. and Y.L. wrote the paper.

Notes

The authors declare the following competing financial interest(s): Y.L. is a professor of Bioscience at Hubei University and a scientific advisor to BravoVax. The regents of Wuhan Polytechnic University and BravoVax have one patent pending for CRISPR-Cas12a detection technologies, on which professor

https://doi.org/10.1021/acssensors.6c01202
ACS Sens. XXXX, XXX, XXX–XXX

Downloaded from pubs.acs.org/ascelj/article-pdf/doi/10.1021/acssensors.6c01202/6604899/se-2026-01202n.pdf by XIAMEN UNIV user on 23 August 2026

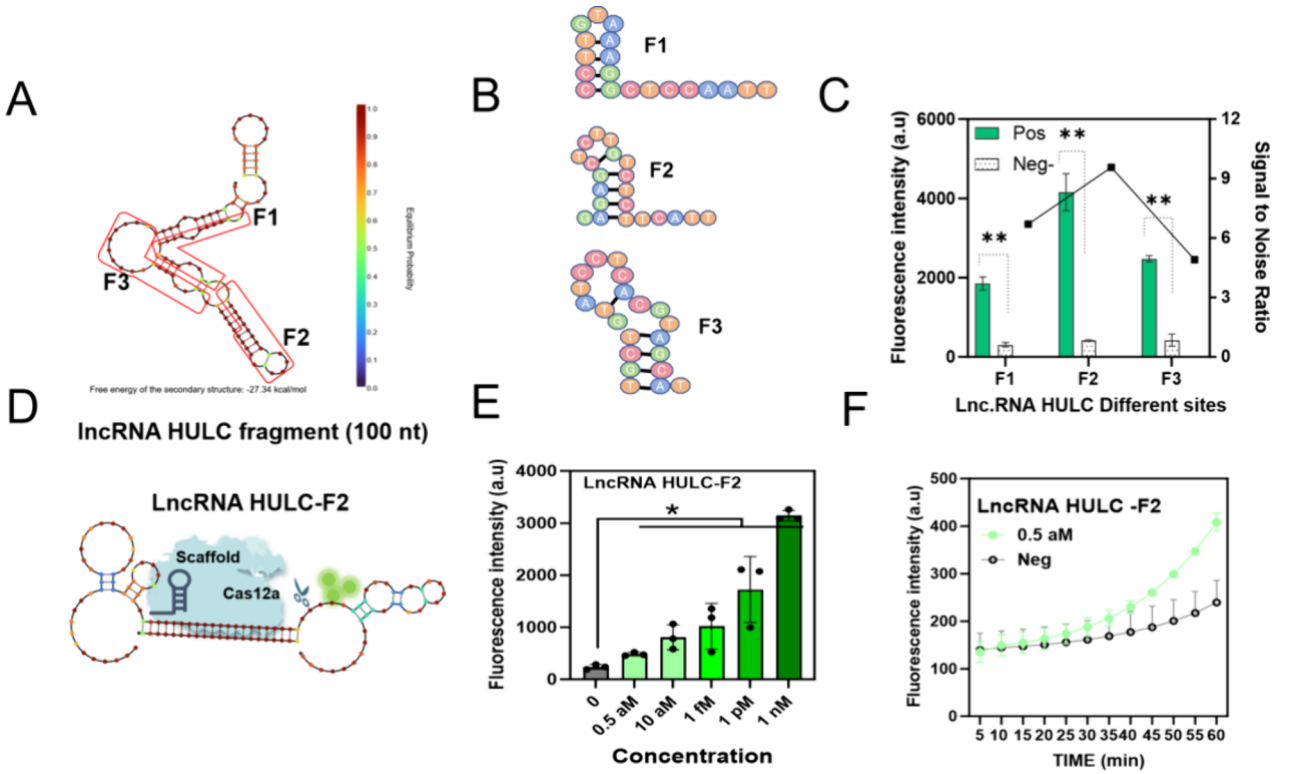


Figure 6. Detecting lncRNA HULC using RTLC. (A) Secondary structure diagram of the lncRNA HULC (100 nt), drawn by NUPACK (https://nupack.org/). (B) Schematic structures of DNA activators targeting three different sites of lncRNA HULC; (C) Detection results for the F1, F2, and F3 sites; (D) Schematic diagram of detection targeting the F2 site; (E) End-point fluorescence intensities for different concentrations of lncRNA HULC at 60 min. (F) Real-time fluorescence kinetic curve for 0.5 aM lncRNA HULC over 60 min. Data are presented as mean ± SD ($n = 3$). "Pos" and "Neg" stand for positive and negative, respectively. Statistical significance is indicated as follows: *$P < 0.05$, **$P < 0.01$, ***$P < 0.001$, ****$P < 0.0001$, based on a two-tailed P value from an unpaired *t*-test.

Y.L. and J.Q. are inventors. The remaining authors declare no competing interests.

■ ACKNOWLEDGMENTS

This work was supported by the Science and Technology Innovation Talent Plan of Hubei Province (2023DJC136), the Natural Science Foundation of Hubei Province (2025AFB825), the Natural Science Foundation of Wuhan (2026040301020081), the Emerging Interdisciplinary Research Funding of WHPU (No. WHPU-EIRF-2606), the Faculty Research Development Program of the School of Life Science and Technology, Wuhan Polytechnic University (grant No. WHPUSK2025-26).

■ REFERENCES

(1) Han, X.; Li, J.; Chen, Y.; Li, Y.; Xu, Y.; Ying, B.; Shang, H. SARS-CoV-2 nucleic acid testing is China's key pillar of COVID-19 containment. *Lancet* **2022**, *399* (10336), 1690–1691.

(2) Yi, B.; Zhou, B.; Zhou, D.; Yang, L.; Xu, H. CRISPR/Cas-powered nucleic acid amplification and amplification-free biosensors for public safety detection: Principles, advances and prospects. *Biotechnol. Adv.* **2025**, *83*, 108609.

(3) Li, H.; Xie, Y.; Chen, F.; Bai, H.; Xiu, L.; Zhou, X.; Guo, X.; Hu, Q.; Yin, K. Amplification-free CRISPR/Cas detection technology: challenges, strategies, and perspectives. *Chem. Soc. Rev.* **2023**, *52* (1), 361–382.

(4) Kaminski, M. M.; Abudayyeh, O. O.; Gootenberg, J. S.; Zhang, F.; Collins, J. J. CRISPR-based diagnostics. *Nat. Biomed. Eng.* **2021**, *5* (7), 643–656.

(5) Huyke, D. A.; Ramachandran, A.; Bashkirov, V. I.; Kotseroglou, E. K.; Kotseroglou, T.; Santiago, J. G. Enzyme Kinetics and Detector Sensitivity Determine Limits of Detection of Amplification-Free CRISPR-Cas12 and CRISPR-Cas13 Diagnostics. *Anal. Chem.* **2022**, *94* (27), 9826–9834.

(6) Hu, M.; Wang, Y.; Qi, W.; Zhang, Y.; Sun, J.; Cheng, M.; Zhou, X. Photocontrolled Programmable Enzymatic Cascade for Robust CRISPR Diagnostics. *J. Am. Chem. Soc.* **2025**, *147* (34), 31004–31015.

(7) Gootenberg, J. S.; Abudayyeh, O. O.; Lee, J. W.; Essletzbichler, P.; Dy, A. J.; Joung, J.; Verdine, V.; Donghia, N.; Daringer, N. M.; Freije, C. A.; Myhrvold, C.; Bhattacharyya, R. P.; Livny, J.; Regev, A.; Koonin, E. V.; Hung, D. T.; Sabeti, P. C.; Collins, J. J.; Zhang, F. Nucleic acid detection with CRISPR-Cas13a/C2c2. *Science* **2017**, *356* (6336), 438–442.

(8) Broughton, J. P.; Deng, X.; Yu, G.; Fasching, C. L.; Servellita, V.; Singh, J.; Miao, X.; Streithorst, J. A.; Granados, A.; Sotomayor-Gonzalez, A.; Zorn, K.; Gopez, A.; Hsu, E.; Gu, W.; Miller, S.; Pan, C. Y.; Guevara, H.; Wadford, D. A.; Chen, J. S.; Chiu, C. Y. CRISPR-Cas12-based detection of SARS-CoV-2. *Nat. Biotechnol.* **2020**, *38* (7), 870–874.

(9) Li, S. Y.; Cheng, Q. X.; Wang, J. M.; Li, X. Y.; Zhang, Z. L.; Gao, S.; Cao, R. B.; Zhao, G. P.; Wang, J. CRISPR-Cas12a-assisted nucleic acid detection. *Cell Discov.* **2018**, *4*, 20.

(10) Han, J.; Kim, S.; Kim, S.; Lee, E. S.; Cha, B. S.; Park, J. S.; Shin, J.; Jang, Y.; Park, K. S. Cas12a-based primer production enables isothermal amplification for nucleic acid detection. *Sens. Actuators B Chem.* **2023**, *381*, 133401.

Downloaded from pubs.acs.org/ascefj/article-pdf/doi/10.1021/acssensors.6c01202/6604899/se-2026-01202n.pdf by XIAMEN UNIV user on 23 August 2026

https://doi.org/10.1021/acssensors.6c01202
ACS Sens. XXXX, XXX, XXX–XXX

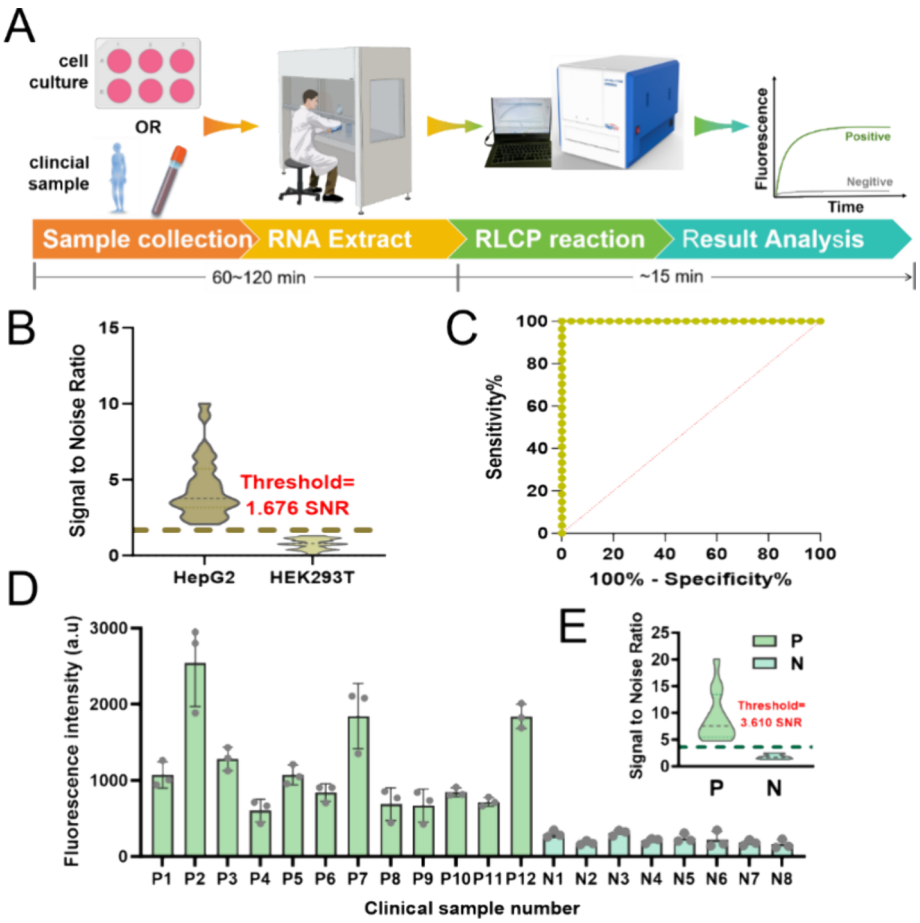


Figure 7. Development of the RTLC assay for practical applications. (A) Schematic workflow of RTLC in real-world testing; (B) determination of the decision threshold SNR (1.676) for RTLC; (C) ROC curve analysis of HepG2 cells using RTLC, demonstrating 100% sensitivity and 100% specificity; (D) detection of miR-21 in blood samples from patients and healthy individuals via RTLC; and (E) signal-to-noise ratio results from clinical samples shown in Figure 7D. Data are presented as mean ± SD ($n = 3$).

(11) Han, J.; Shin, J.; Lee, E. S.; Cha, B. S.; Kim, S.; Jang, Y.; Kim, S.; Park, K. S. Cas12a/blocker DNA-based multiplex nucleic acid detection system for diagnosis of high-risk human papillomavirus infection. *Biosens. Bioelectron.* **2023**, *232*, 115323.
(12) Kim, J.; Lee, G. H.; Nam, D.; Park, K. S. Enhancing multiplex detection capabilities of the Cas12a/blocker DNA system. *Talanta* **2025**, *281*, 126864.
(13) Wang, Z.; Wu, Y.; Wang, Z.; Zhang, S.; Liu, H.; Nie, Y.; Chen, K.; Huang, Y.; Zhou, Y.; Cao, Y.; Sun, L.; Hao, R. crRNA scaffold remodeling controls CRISPR–Cas12a activity for enhanced performance. *Nucleic Acids Res.* **2026**, *54* (5), gkag167.
(14) Zhang, D.; Yan, Y.; Que, H.; Yang, T.; Cheng, X.; Ding, S.; Zhang, X.; Cheng, W. CRISPR/Cas12a-Mediated Interfacial Cleaving of Hairpin DNA Reporter for Electrochemical Nucleic Acid Sensing. *ACS Sens.* **2020**, *5* (2), 557–562.
(15) Lee, S.; Nam, D.; Park, J. S.; Kim, S.; Lee, E. S.; Cha, B. S.; Park, K. S. Highly Efficient DNA Reporter for CRISPR/Cas12a-Based Specific and Sensitive Biosensor. *BioChip J.* **2022**, *16* (4), 463–470.
(16) Shi, K.; Xie, S.; Tian, R.; Wang, S.; Lu, Q.; Gao, D.; Lei, C.; Zhu, H.; Nie, Z. A CRISPR-Cas autocatalysis-driven feedback amplification network for supersensitive DNA diagnostics. *Sci. Adv.* **2021**, *7* (5), eabc7802.
(17) Sun, K.; Pu, L.; Chen, C.; Chen, M.; Li, K.; Li, X.; Li, H.; Geng, J. An autocatalytic CRISPR-Cas amplification effect propelled by the LNA-modified split activators for DNA sensing. *Nucleic Acids Res.* **2024**, *52* (7), e39.
(18) Fei, J.; Ha, T. Watching DNA breath one molecule at a time. *Proc. Natl. Acad. Sci. U. S. A.* **2013**, *110* (43), 17173–17174.
(19) Jose, D.; Weitzel, S. E.; von Hippel, P. H. Breathing fluctuations in position-specific DNA base pairs are involved in regulating helicase movement into the replication fork. *Proc. Natl. Acad. Sci. U. S. A.* **2012**, *109* (36), 14428–14433.
(20) Lim, J.; Van, A. B.; Koprowski, K.; Wester, M.; Valera, E.; Bashir, R. Amplification-free, OR-gated CRISPR-Cascade reaction for pathogen detection in blood samples. *Proc. Natl. Acad. Sci. U. S. A.* **2025**, *122* (11), e2420166122.
(21) Chen, Y.; Zhang, Y.; Luo, S.; Yang, X.; Liu, C.; Zhang, Q.; Liu, Y.; Zhang, X. Foldback-crRNA-Enhanced CRISPR/Cas13a System (FCECas13a) Enables Direct Detection of Ultrashort sncRNA. *Anal. Chem.* **2023**, *95* (42), 15606–15613.
(22) Yang, H.; Patel, D. J. Structures, mechanisms and applications of RNA-centric CRISPR-Cas13. *Nat. Chem. Biol.* **2024**, *20* (6), 673–688.
(23) Fozouni, P.; Son, S.; Díaz de León Derby, M.; Knott, G. J.; Gray, C. N.; D'Ambrosio, M. V.; Zhao, C.; Switz, N. A.; Kumar, G. R.; Stephens, S. I.; Boehm, D.; Tsou, C. L.; Shu, J.; Bhuiya, A.; Armstrong, M.; Harris, A. R.; Chen, P. Y.; Osterloh, J. M.; Meyer-Franke, A.; Joehnk, B.; Walcott, K.; Sil, A.; Langelier, C.; Pollard, K. S.; Crawford, E. D.; Puschnik, A. S.; Phelps, M.; Kistler, A.; DeRisi, J. L.; Doudna, J. A.; Fletcher, D. A.; Ott, M. Amplification-free detection of SARS-CoV-2 with CRISPR-Cas13a and mobile phone microscopy. *Cell* **2021**, *184* (2), 323–333.e9.

Downloaded from pubs.acs.org/ascefj/article-pdf/doi/10.1021/acssensors.6c01202/6604899/se-2026-01202n.pdf by XIAMEN UNIV user on 23 August 2026

https://doi.org/10.1021/acssensors.6c01202
ACS Sens. XXXX, XXX, XXX–XXX

(24) Chen, Y.; Wang, X.; Zhang, J.; Jiang, Q.; Qiao, B.; He, B.; Yin, W.; Qiao, J.; Liu, Y. Split crRNA with CRISPR-Cas12a enabling highly sensitive and multiplexed detection of RNA and DNA. *Nat. Commun.* **2024**, *15* (1), 8342.
(25) Zhang, J.; Yin, W.; Jiang, Q.; Mao, W.; Deng, W.; Jin, S.; Wang, X.; He, R.; Qiao, J.; Liu, Y. Precise amplification-free detection of highly structured RNA with an enhanced SCas12a assay. *Commun. Biol.* **2025**, *8* (1), 366.
(26) Rananaware, S. R.; Vesco, E. K.; Shoemaker, G. M.; Anekar, S. S.; Sandoval, L. S. W.; Meister, K. S.; Macaluso, N. C.; Nguyen, L. T.; Jain, P. K. Programmable RNA detection with CRISPR-Cas12a. *Nat. Commun.* **2023**, *14* (1), 5409.
(27) Nie, Y. G.; Zhang, H. S.; Su, M.; Zha, C. J.; Yang, K.; Ying, Z. M. Proximity-Inducible CRISPR/Cas12a Activity by Scaffold RNA Assembly for Sensing Applications. *Anal. Chem.* **2025**, *97* (50), 28088–28097.
(28) Zha, C. J.; Z., H.; Su, M.; Nie, Y. G.; Ying, Z. M. Intrinsic crRNA Scaffold Dynamic Reassembly Powered Cas12a Cascade Amplification for Multiplexed Detection. *Anal. Chem.* **2026**, *98* (5), 4372–4381.
(29) Zhu, J.; Wang, C.; Huang, T.; Zeng, L.; Niu, Q.; Huang, X.; Chen, H.; Jiang, M.; Deng, B.; Yan, Y.; Liu, X.; Chen, J.; Xie, Y.; Shen, J.; Chen, W.; Gao, Y.; Chen, K.; Lin, X.; Zeng, L.; Li, B.; Song, Y.; Zhu, J.; Li, B. Rapid Detection and Purification of Extracellular Vesicles for Hepatocellular Carcinoma Screening Using a Plasmonic Metasurface Integrated with the Kolmogorov–Arnold Network. *ACS Nano* **2025**, *19* (49), 41557–41570.
(30) Zhu, J.; Xiao, Y.; Huang, X.; Niu, Q.; Zeng, L.; Lin, S.; Jiang, M.; Huang, T.; Chen, H.; Xie, Y.; Gao, Y.; Chen, W.; Yan, Y.; Shen, J.; Chen, K.; Dai, Y.; Zhang, Z.; Zeng, L.; Chen, Y.; Li, B.; Zhu, J.; Li, B. Deep Learning-Powered Nanoplasmonic Biosensing Approach Enables Ultrasensitive Extracellular Vesicles Profiling for Cancer Screening. *Adv. Sci. (Weinh)* **2026**, *13* (2), e11337.
(31) Xu, T.; Zhang, Y.; Li, S.; Dai, C.; Wei, H.; Chen, D.; Zhao, Y.; Liu, H.; Li, D.; Chen, P.; Liu, B. F.; Tian, Y. Deep Learning-Enhanced Hand-Driven Microfluidic Chip for Multiplexed Nucleic Acid Detection Based on RPA/CRISPR. *Adv. Sci. (Weinh)* **2025**, *12* (21), e2414918.
(32) Wu, J.; Gao, P.; Shi, Y.; Zhang, C.; Tong, X.; Fan, H.; Zhou, X.; Zhang, Y.; Yin, H. Characterization of a thermostable Cas12a ortholog. *Cell Insight* **2023**, *2* (6), 100126.
(33) Nalefski, E. A.; Patel, N.; Leung, P. J. Y.; Islam, Z.; Kooistra, R. M.; Parikh, I.; Marion, E.; Knott, G. J.; Doudna, J. A.; Le Ny, A. M.; Madan, D. Kinetic analysis of Cas12a and Cas13a RNA-Guided nucleases for development of improved CRISPR-Based diagnostics. *iScience* **2021**, *24* (9), 102996.
(34) Hu, M.; Cheng, X.; Wu, T. Modular CRISPR/Cas12a synergistic activation platform for detection and logic operations. *Nucleic Acids Res.* **2024**, *52* (12), 7384–7396.
(35) Fratczak, A.; Kierzek, R.; Kierzek, E. LNA-modified primers drastically improve hybridization to target RNA and reverse transcription. *Biochemistry* **2009**, *48* (3), 514–516.
(36) Varkonyi-Gasic, E.; Wu, R.; Wood, M.; Walton, E. F.; Hellens, R. P. Protocol: a highly sensitive RT-PCR method for detection and quantification of microRNAs. *Plant Methods* **2007**, *3*, 12.
(37) Yin, N.; Yu, H.; Zhang, L.; Luo, F.; Wang, W.; Han, X.; He, Y.; Zhang, Y.; Wu, Y.; Pu, J.; Feng, T.; Yang, G.; Chen, T.; Xie, G. Regulation of CRISPR trans-cleavage activity by an overhanging activator. *Nucleic Acids Res.* **2025**, *53* (4), gkaf117.
(38) Zhang, Y.; Xiang, Y.; Hou, D.; Fang, L.; Cai, S.; Zhang, J.; Wang, Y.; Jiang, Y.; Liu, B.; Bai, J.; Ding, Y.; Fang, J.; Chen, S.; Liu, X.; Ren, X. A one-pot method for universal Dengue virus detection by combining RT-RPA amplification and CRISPR/Cas12a assay. *BMC Microbiol.* **2025**, *25* (1), 163.
(39) Aman, R.; Mahas, A.; Marsic, T.; Hassan, N.; Mahfouz, M. M. Efficient, Rapid, and Sensitive Detection of Plant RNA Viruses With One-Pot RT-RPA-CRISPR/Cas12a Assay. *Front. Microbiol.* **2020**, *11*, 610872.
(40) Li, Z.; Zhao, W.; Ma, S.; Li, Z.; Yao, Y.; Fei, T. A chemical-enhanced system for CRISPR-Based nucleic acid detection. *Biosens. Bioelectron.* **2021**, *192*, 113493.
(41) Son, H.; Park, J.; Hwang, I.; Jung, Y.; Bae, S.; Lee, S. $Mg^{(2+)}$-dependent conformational rearrangements of CRISPR-Cas12a R-loop complex are mandatory for complete double-stranded DNA cleavage. *Proc. Natl. Acad. Sci. U. S. A.* **2021**, *118* (49), e2113747118.
(42) Whiting, S. H.; Champoux, J. J. Strand displacement synthesis capability of Moloney murine leukemia virus reverse transcriptase. *J. Virol.* **1994**, *68* (8), 4747–4758.
(43) Bhan, A.; Soleimani, M.; Mandal, S. S. Long Noncoding RNA and Cancer: A New Paradigm. *Cancer Res.* **2017**, *77* (15), 3965–3981.
(44) Yu, K.; Jin, Y.; Zhou, Y.; Xu, Q. Long non-coding RNA in hepatocellular carcinoma: mechanistic insights and therapeutic perspectives. *Cell. Oncol. (Dordr.)* **2025**, *48* (6), 1677–1692.
(45) Panzitt, K.; Tschernatsch, M. M.; Guelly, C.; Moustafa, T.; Stradner, M.; Strohmaier, H. M.; Buck, C. R.; Denk, H.; Schroeder, R.; Trauner, M.; Zatloukal, K. Characterization of HULC, a novel gene with striking up-regulation in hepatocellular carcinoma, as noncoding RNA. *Gastroenterology* **2007**, *132* (1), 330–342.
(46) Ng, E. K.; Chong, W. W.; Jin, H.; Lam, E. K.; Shin, V. Y.; Yu, J.; Poon, T. C.; Ng, S. S.; Sung, J. J. Differential expression of microRNAs in plasma of patients with colorectal cancer: a potential marker for colorectal cancer screening. *Gut* **2009**, *58* (10), 1375–1381.

Downloaded from pubs.acs.org/ascelj/article-pdf/doi/10.1021/acssensors.6c01202/6604899/se-2026-01202n.pdf by XIAMEN UNIV user on 23 August 2026

https://doi.org/10.1021/acssensors.6c01202
ACS Sens. XXXX, XXX, XXX–XXX